
This copy is for your personal, non-commercial use only.

If you wish to distribute this article to others, you can order high-quality copies for your colleagues, clients, or customers by [clicking here](#).

Permission to republish or repurpose articles or portions of articles can be obtained by following the guidelines [here](#).

The following resources related to this article are available online at www.sciencemag.org (this information is current as of July 7, 2011):

Updated information and services, including high-resolution figures, can be found in the online version of this article at:

<http://www.sciencemag.org/content/296/5576/2195.full.html>

This article **cites 19 articles**, 3 of which can be accessed free:

<http://www.sciencemag.org/content/296/5576/2195.full.html#ref-list-1>

This article has been **cited by** 34 article(s) on the ISI Web of Science

This article appears in the following **subject collections**:

Physics

<http://www.sciencemag.org/cgi/collection/physics>

should be possible to transfer condensates containing more than 10^7 atoms and accumulate more than 10^8 atoms in the continuous source. This would be larger than any condensate produced thus far using the standard combination of laser cooling and evaporative cooling.

Outlook: Condensate Phase and CW Atom Lasers

An interesting aspect of the continuous BEC is its phase. So far, the phase evolution of condensates have been traced only over sub-second time intervals (16, 17). A measurement of the phase of the continuous BEC source would require separating a small part of the source as a local oscillator and maintaining its phase over the duration of the entire experiment. Although this seems to be out of the reach of current experiments, one may speculate on how the phase would evolve during replenishment of a condensate. The freshly prepared condensates have a random phase relative to the condensate in the reservoir trap, and therefore, in the current experiment, the phase of the source after replenishment will be random relative to the phase before the merger. However, in the limit of a large continuously held condensate merging with a smaller condensate, one would expect the phase of the large condensate to dominate. Each replenishment would create some excitation, and relaxation would result in a condensate with a slightly modified phase, a process reminiscent of phase diffusion in an optical laser. This and other aspects of the merger warrant future theoretical studies, such as of phase coherence, dissipation, and the role of quantum tunnelling during the merger.

In principle, it would be possible to re-

plenish a stationary continuous BEC source with an incoming moving condensate using phase coherent amplification (18, 19). While a stationary source overlaps with a moving condensate dressed by a laser beam, light scattering could phase-coherently amplify the condensate in the reservoir using atoms from the moving condensate. In this scheme, the necessary dissipation is provided by the optical pumping process.

All atom lasers to date (16, 20–22) have operated in a pulsed mode. Coherent streams of atoms were generated until a single condensate was completely depleted. Using our continuous BEC source, one could implement CW-outcoupling and create a truly continuous atom laser. By varying the intensity of the outcoupling field with some feedback, one could compensate for the cyclic variation in the density of the continuous BEC source, thereby outcoupling a continuous atomic-matter wave with constant amplitude. The optical analog of this configuration would be a pulsed laser that delivers photons to an external storage cavity from which a CW laser beam is then extracted. Although a long storage time for photons is not feasible, it is straightforward for atoms. Furthermore, the merger of several pulses requires dissipation and cooling, and therefore interactions, which are present between atoms, but not between photons.

Conclusion

In this work, techniques were developed to produce a new condensate in proximity to another condensate and to merge condensates. We have used these techniques to create a continuous source of Bose-Einstein condensed atoms.

References and Notes

1. W. Ketterle, D. Durfee, D. Stamper-Kurn, *Proceedings of the International School of Physics-Enrico Fermi*, M. Inguscio, S. Stringari, C. Wieman, Eds. (IOS Press, Amsterdam, 1999), pp. 67–176.
2. F. Dalfovo, S. Giorgini, L. P. Pitaevskii, S. Stringari, *Rev. Mod. Phys.* **71**, 463 (1999).
3. T. H. Maiman, *Nature* **187**, 493 (1960).
4. A. Javan, W. R. Bennett, D. Herriott, *Phys. Rev. Lett.* **6**, 106 (1961).
5. R. J. C. Spreeuw, T. Pfau, U. Janicke, M. Wilkens, *Europhys. Lett.* **32**, 469 (1995).
6. M. Olshanii, Y. Castin, J. Dalibard, *Proceedings of the 12th International Conference on Laser Spectroscopy*, M. Inguscio, M. Allegrini, A. Sasso, Eds. (World Scientific, New York, 1996), pp. 7–12.
7. E. Mandonnet *et al.*, *Eur. Phys. J. D* **10**, 9 (2000).
8. B. K. Teo, G. Raithel, *Phys. Rev. A* **63**, 031492(R) (2001).
9. P. Cren, C. F. Roos, A. Aclan, J. Dalibard, D. Guéry-Odelin (2002). Preprint, <http://xxx.lanl.gov/abs/cond-mat/0203618>.
10. W. Rooijackers, M. Vengalattore, R. Conroy, M. Prentiss, personal communication.
11. T. L. Gustavson *et al.*, *Phys. Rev. Lett.* **88**, 020401 (2002).
12. A. E. Leanhardt *et al.*, (2002). Preprint, <http://xxx.lanl.gov/abs/cond-mat/0203214>.
13. D. M. Stamper-Kurn *et al.*, *Phys. Rev. Lett.* **80**, 2027 (1998).
14. A. Görlitz, *et al.*, *Phys. Rev. Lett.* **87**, 130402 (2001).
15. A. Görlitz *et al.*, in preparation.
16. B. Anderson, M. Kasevich, *Science* **282**, 1686 (1998).
17. D. S. Hall, M. R. Matthews, C. E. Wieman, E. A. Cornell, *Phys. Rev. Lett.* **81**, 1543 (1998).
18. S. Inouye *et al.*, *Nature* **402**, 641 (1999).
19. M. Kozuma *et al.*, *Science* **286**, 2309 (1999).
20. M.-O. Mewes *et al.*, *Phys. Rev. Lett.* **78**, 582 (1997).
21. I. Bloch, T. W. Hänsch, T. Esslinger, *Phys. Rev. Lett.* **82**, 3008 (1999).
22. E. Hagley *et al.*, *Science* **283**, 1706 (1999).
23. Funded by the Office of Naval Research, NSF, Army Research Office, NASA, and the David and Lucile Packard Foundation. A.E.L. acknowledges additional support from NSF. We thank Z. Hadzibabic for a critical reading of the manuscript.

12 April 2002; accepted 8 May 2002

REPORTS

Coherent Spin Oscillations in a Disordered Magnet

S. Ghosh,¹ R. Parthasarathy,¹ T. F. Rosenbaum,^{1*} G. Aeppli²

Most materials freeze when cooled to sufficiently low temperature. We find that magnetic dipoles randomly distributed in a solid matrix condense into a spin liquid with spectral properties on cooling that are the diametric opposite of those for conventional glasses. Measurements of the nonlinear magnetic dynamics in the low-temperature liquid reveal the presence of coherent spin oscillations composed of hundreds of spins with lifetimes of up to 10 seconds. These excitations can be labeled by frequency and manipulated by the magnetic fields from a loop of wire and can permit the encoding of information at multiple frequencies simultaneously.

Magnetic solids offer arrays of quantum degrees of freedom, or spins, that interact with each other in a manner and strength ranging from the long-range ferromagnetism of iron and nickel to the nano-antiferromagnetism of vortices in high-temperature superconduc-

tors. Unfortunately, there is a large barrier to exploiting quantum effects in magnetic solids; namely, the rarity of coherence effects that can be simply manipulated and observed (1). In particular, it is difficult to create the magnetization oscillations corresponding to

prepared superpositions of states, which are so straightforwardly created in liquid-phase nuclear magnetic resonance experiments. The “decoherence” for the solid magnets is generally attributed to disorder and to the coupling of the electronic spins to other degrees of freedom, such as nuclear spins, atomic motion, and conduction electrons. Here we describe coherence effects in a magnet, $\text{LiHo}_{0.045}\text{Y}_{0.955}\text{F}_4$, which is highly disordered but does not suffer from coupling to either conduction electrons or to atomic motions, because it is a strongly ionic insulator with the spins derived from small, nonoverlapping electronic orbitals.

¹The James Franck Institute and Department of Physics, The University of Chicago, Chicago, IL 60637, USA. ²NEC Research Institute, 4 Independence Way, Princeton, NJ 08540, USA.

*To whom correspondence should be addressed. E-mail: t-rosenbaum@uchicago.edu

Pure LiHoF₄ is a ferromagnet because of its crystal structure and the dominant role of the magnetic dipole interaction (2) between the unpaired f electrons of the Ho³⁺ ions. When nonmagnetic Y³⁺ ions are randomly substituted for the Ho³⁺ ions, the fact that the anisotropic dipolar interaction can be antiferromagnetic as well as ferromagnetic begins to matter. The result is that with decreasing dipole concentration, the ferromagnetism is first suppressed and then destroyed, only to be replaced by conventional spin freezing (3), analogous to the freezing of liquids into glasses. In a glass, barriers to relaxation proliferate with decreasing tempera-

ture, and the system response slows and broadens. A surprising result of an early study (4) was that, contrary to intuition as well as to theory (5), further dilution of Ho by Y eliminated the glassy freezing in favor of a state that becomes progressively less glassy on cooling to temperatures as low as tens of millikelvins. The “antiglass” state for LiHo_{0.045}Y_{0.955}F₄ is the host for the coherence effects that we have discovered.

We cooled a single crystal of LiHo_{0.045}Y_{0.955}F₄ with dimensions of 1.0 cm by 0.5 cm by 0.5 cm to millikelvin temperatures by using a helium dilution refrigerator. The energy scale

is set by the nearest-neighbor dipole interaction strength, $J_{nn} = 1.2$ K. Internal crystal fields force the randomly distributed Ho dipoles to point along the long crystalline *c* axis, providing a one-dimensional Ising spin symmetry. We focus on how the sample magnetization responds to oscillating external magnetic fields along the *c* axis of varying amplitudes h_{ac} (6). Ordinary disordered magnets respond to a changing external field via exponential relaxation $\exp(-t/\tau)$, where τ is a characteristic time. When transformed into the frequency domain, this corresponds to the Debye form (7), $\chi(f) = \chi_0/(1 + 2\pi i f \tau)$. Glasses are typically described by a distribution of relaxation times, resulting in a response function that is the superposition of Debye forms for the times τ in the distribution. The outcome is a spectrum that becomes progressively wider on cooling (3, 8).

We plot $\chi''(f)$ for LiHo_{0.045}Y_{0.955}F₄ over five decades in f at seven different temperatures (Fig. 1). Spin relaxation becomes slower at low temperature, and the spectral response moves to lower f with decreasing T . The typical frequency for spin reorientation, given by the peak in $\chi''(f)$, falls below 1 Hz for $T < 0.090$ K. Even while the overall dynamics slow, the spectrum continues to narrow down to the lowest T , opposite to the behavior observed in regular dielectric and magnetic glasses. The response function actually becomes narrower than Debye: 0.8 decades at $T = 0.050$ K as compared to the theoretical limit of 1.14 decades full width at half maximum for a single relaxation time. Moreover, the distribution of relaxation times becomes severely truncated at low frequencies (long times) as an apparent gap (9, 10) opens in the spectrum below a cutoff f varying between 1 and 0.1 Hz on cooling from 0.120 to 0.050 K.

The sharpened spectra and the appearance of a gap imply that we are dealing with a set of oscillators rather than a distribution of relaxation times. An important consequence is that we should be able to address the oscillators individually via the technique of resonant hole burning, exactly as for optical systems. Hole burning consists of saturating an inhomogeneously broadened resonance line at its resonance frequency, bleaching the system response at that frequency (11). The first signature of bleaching is saturation of the signal amplitude with excitation field. Figure 2A demonstrates exactly such an effect for a 5-Hz excitation applied to our disordered magnet at $T = 0.110$ K. In addition, Fig. 2B shows that the phase lag between the signal and the excitation essentially vanishes on crossing between the linear low-field and saturated high-field regimes. Thus, dissipation decreases sharply when the excitation field is raised.

The resonant character of the high-field, nondissipative regime is established by simultaneously applying a high-amplitude pump and a small-amplitude probe along the Ising axis (Fig. 2, inset). The pump frequency is kept

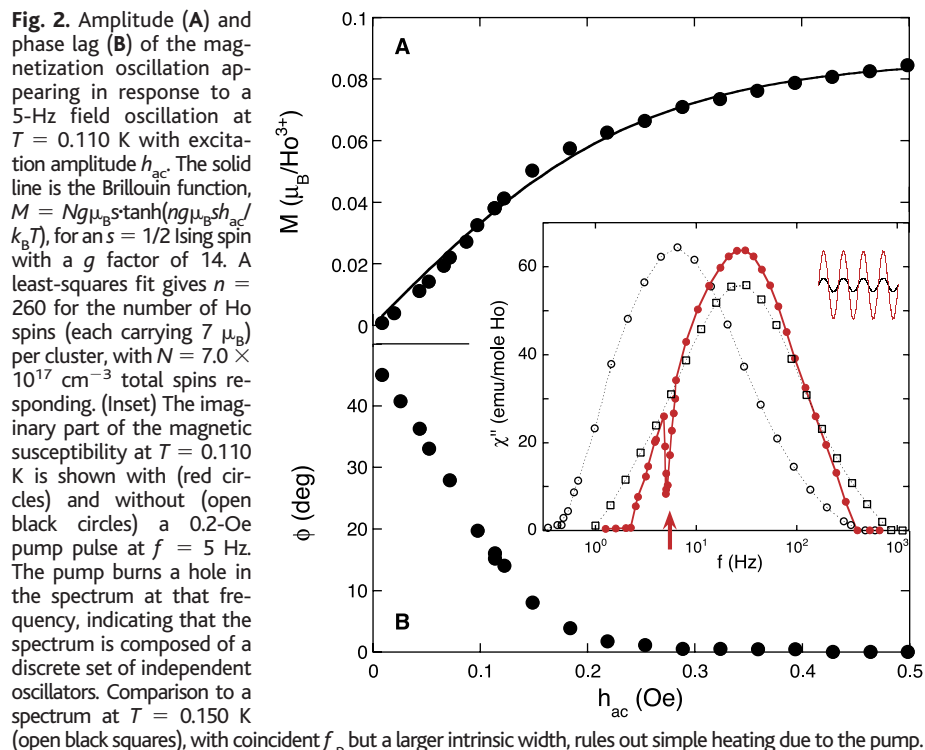
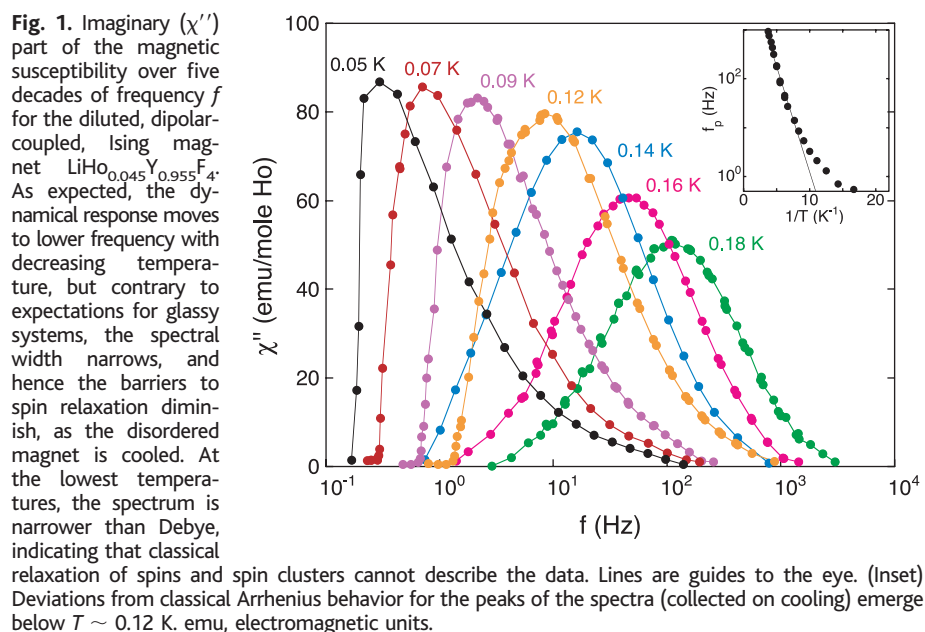


Fig. 1. Imaginary (χ'') part of the magnetic susceptibility over five decades of frequency f for the diluted, dipolar-coupled, Ising magnet LiHo_{0.045}Y_{0.955}F₄. As expected, the dynamical response moves to lower frequency with decreasing temperature, but contrary to expectations for glassy systems, the spectral width narrows, and hence the barriers to spin relaxation diminish, as the disordered magnet is cooled. At the lowest temperatures, the spectrum is narrower than Debye, indicating that classical relaxation of spins and spin clusters cannot describe the data. Lines are guides to the eye. (Inset) Deviations from classical Arrhenius behavior for the peaks of the spectra (collected on cooling) emerge below $T \sim 0.12$ K. emu, electromagnetic units.

Fig. 2. Amplitude (A) and phase lag (B) of the magnetization oscillation appearing in response to a 5-Hz field oscillation at $T = 0.110$ K with excitation amplitude h_{ac} . The solid line is the Brillouin function, $M = Ng\mu_B s \tanh(ng\mu_B s h_{ac} / k_B T)$, for an $s = 1/2$ Ising spin with a g factor of 14. A least-squares fit gives $n = 260$ for the number of Ho spins (each carrying $7 \mu_B$) per cluster, with $N = 7.0 \times 10^{17} \text{ cm}^{-3}$ total spins responding. (Inset) The imaginary part of the magnetic susceptibility at $T = 0.110$ K is shown with (red circles) and without (open black circles) a 0.2-Oe pump pulse at $f = 5$ Hz. The pump burns a hole in the spectrum at that frequency, indicating that the spectrum is composed of a discrete set of independent oscillators. Comparison to a spectrum at $T = 0.150$ K (open black squares), with coincident f_p but a larger intrinsic width, rules out simple heating due to the pump.

fixed whereas that of the probe is varied to obtain the spectrum. The pump has several important effects. First, the spectrum's peak shifts from 6 to 27 Hz. Second, whereas the spectral shape below the peak remains unchanged on the logarithmic-linear scale used to plot the data, it narrows above the peak. Furthermore, the spectrum is considerably narrower than that found when the temperature is raised to 0.150 K, to obtain (in the small-probe amplitude limit) the same peak frequency, and we conclude that the pump is not simply heating the sample. Finally, and most dramatically, the pump amplitude of merely 0.2 Oe (five times the probe amplitude $h_{ac} = 0.04$ Oe) at $f = 5$ Hz carves out a hole in $\chi''(f)$ that removes 75% of the original signal. No other portion of the spectrum is similarly affected. Varying the pump frequency burns holes of similar depth and width for any given $f < f_p$. A macroscopic number of spins defines any such independent state: integrating $\chi''(f)/f$ over f and normalizing by T yields $\sim 7.5 \times 10^{17}$ spins cm^{-3} transparent to the probe, which is fully 1.5% of the total number accessible at $T = 0.110$ K.

If the oscillators excited at one resonance frequency are independent from other oscillators in the antighass, then it may be possible to burn holes in parallel at different frequencies. To this end, we substituted a square wave pump for the sinusoidal pump. By Fourier decomposition of the square wave, the substitution is equivalent to applying simultaneous sinusoidal pumps at $f_0, 3f_0, 5f_0, \dots$ with peak-to-peak amplitudes $a_0, a_0/3, a_0/5, \dots$, respectively. In the resultant spectrum (Fig. 3), not only is there a hole at 3 Hz, but there is a second one at 9 Hz, and the latter is about one-third as deep as the first, which is the ratio of excitation amplitudes in the Fourier expansion.

How long can the collective spin excitations maintain coherence against dissipation? We answer this question by looking for free induction decay after applying a pump signal and then shutting it off (Fig. 4, left). The magnetization continues to oscillate at the pump frequency for times very much longer than the 0.2-s oscillation period of the pump. The extent of the free induction decay depends on temperature: The decay time rises from 4 to 10 s on cooling from 0.125 to 0.070 K.

The coherent hole-burning and free induction decay of the magnetic excitations in $\text{LiHo}_{0.045}\text{Y}_{0.955}\text{F}_4$ appear to be derived from a collection of nearly independent oscillators embedded in a spin liquid rather than the relaxational modes responsible for the spectral depletion phenomena seen in conventional magnetic and dielectric solids (12–14). What might these oscillators be? The most natural possibility is that they are magnetic clusters switching between states with up and down polarization. A cluster can be represented as a particle with a single coordinate—its magnetization—moving in a potential with two minima corresponding

to the up and down polarized states (Fig. 4, right). For zero applied field, the minima will be separated by a barrier, and switching between the minima occurs at random intervals because of a combination of thermally activated hopping-over and quantum tunneling through the barrier. In large fields the barrier disappears, and there is only one minimum corresponding to a fully polarized cluster. If the system is driven by a small ac magnetic field, the random barrier hopping and tunneling processes will result in dissipative dynamics, but for high drive amplitudes the motion will be deterministic over a large part of the oscillatory cycle. It is then describable in terms of Newtonian equations and can even become dissipationless (Fig. 2B). The long-term ringing, which we observe subsequently as free induction decay (Fig. 4, left), is perhaps the most striking manifestation of the small dissipation for our spin clusters and

points to a large inertial term that is much larger than the dissipative term in the underlying equations of motion (15).

The origin of nearly dissipationless, non-linear dynamics is no doubt linked to that of the antighass phenomenon. Understanding $\text{LiHo}_{0.045}\text{Y}_{0.955}\text{F}_4$ must require an ingredient that is missing from the theory of randomly distributed classical dipoles, for which a glass transition is anticipated even in the limit of infinite dilution (5). We suspect that the ingredient is quantum mechanics, which can play a role in the dilute system, because the off-diagonal terms in the dipolar interaction can act as spin-flipping transverse fields. For disordered samples with sufficient Ho density to achieve ferromagnetism, these components of the dipolar interaction perpendicular to the Ising axis give rise to quantum mechanical ferromagnetic domain wall tunneling, which survives even in

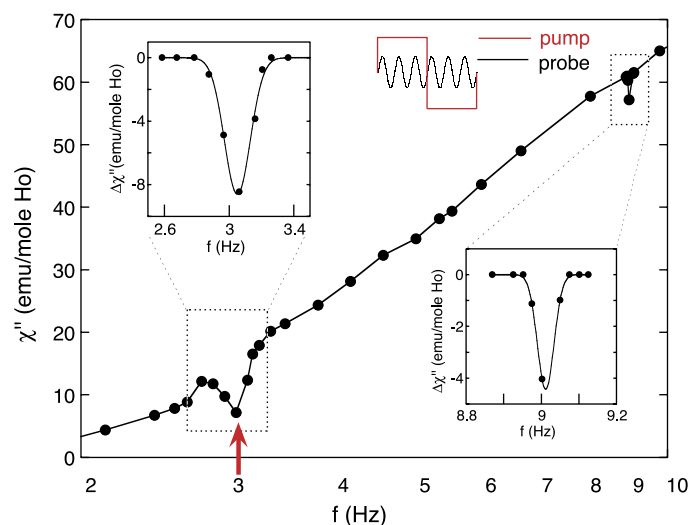


Fig. 3. Multiple holes burned into the spectrum using a square wave pump at $f = 3$ Hz (second Fourier component at $f = 9$ Hz) demonstrate the ability to encode simultaneously multiple bits of information. The hole at $f = 15$ Hz is not shown.

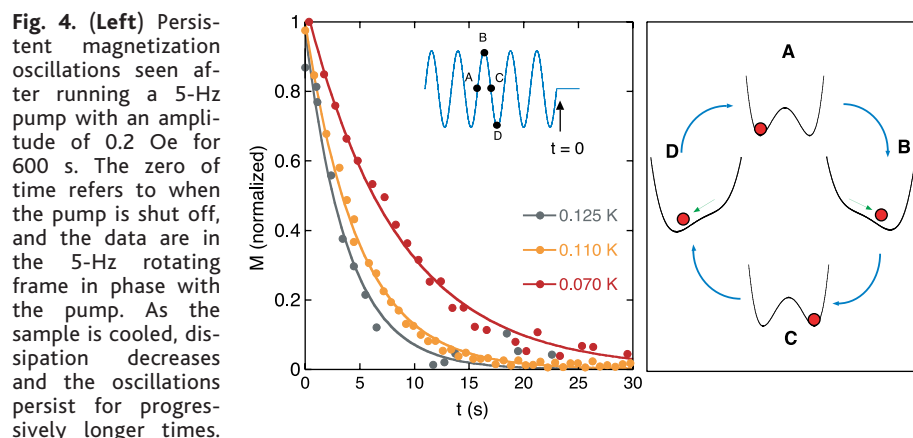


Fig. 4. (Left) Persistent magnetization oscillations seen after running a 5-Hz pump with an amplitude of 0.2 Oe for 600 s. The zero of time refers to when the pump is shut off, and the data are in the 5-Hz rotating frame in phase with the pump. As the sample is cooled, dissipation decreases and the oscillations persist for progressively longer times. (Right) Schematic of spin clusters transiting between their up and down magnetic states at low temperatures during different parts of an ac drive cycle. The cluster magnetization is a degree of freedom subject to a potential, which for zero applied field (A and C) contains two degenerate minima corresponding to up and down states. External fields tilt the potential, until at sufficiently high field, only a single minimum survives, corresponding to magnetization along the field direction (B and D). An ac drive field produces an oscillating potential for the cluster magnetization, resulting in a variety of stochastic effects at low drive amplitudes (19, 20) and saturation and phase-locking effects at high amplitudes.

the limit of zero external transverse field (16). For our dilute crystals, the net outcome is neither a ferromagnetic nor a spin-glass ground state (17, 18) but instead a subdivision of the system into clusters, whose conventional freezing is eventually limited by the quantum fluctuations brought about by the transverse fields from other clusters. The coherent oscillations that we observe could then be thought of as Rabi oscillations of the clusters in the weak transverse mixing fields.

We can use our data to see the crossover to quantum behavior and to measure the size of the clusters. The classical-quantum crossover is apparent from plotting (Fig. 1, inset) the frequency f_p where the imaginary part of the magnetic response peaks against temperature. At high T a thermally activated Arrhenius form, $f_p \sim \exp(-\Delta/k_B T)$, fits the data with a barrier height $\Delta = 1.2 \text{ K} \sim J_{nn}$. For $T < 0.120 \text{ K}$, the sharp gap-like cutoff appears in $\chi''(f)$ and there is a clear deviation from the Arrhenius law in the sense that the dynamics are too fast. We surmise that the dominant effect at low frequencies, drive amplitudes, and temperatures becomes thermally assisted quantum tunneling, with perhaps a role for stochastic synchronization effects (19, 20) in defining the sharp, but nonetheless temperature-dependent, low-frequency cutoff (Fig. 1).

The size of the clusters can be derived from the dependence of the magnetization on external magnetic field. The saturation of the magnetic response in Fig. 2A follows the familiar Brillouin form for Ising spins, $M \sim \tanh(mh_{ac}/k_B T)$. Unlike a simple paramagnet, m here is not the magnetic moment of a single Ho ion (21, 22) but rather the total moment of the spins locked together in the cluster. Analysis of this nonlinear response reveals that the clusters responsible for the saturation and hole burning effects at $T = 0.110 \text{ K}$ and $f = 5 \text{ Hz}$ contain approximately 260 spins. This corresponds to cluster dimensions of approximately six Ho-Ho spacings on a side and a probability of cluster membership of 1% for any given spin in the crystal, comparable to that deduced from the spectral weight carved out by the hole. A cluster of 260 spins, each carrying $7 \mu_B$ and driven at $h_{ac} = 0.5 \text{ Oe}$, sets an effective energy scale $\sim 0.13 \text{ K}$, comparable to the measuring temperature T , the onset temperature for deviations from Arrhenius behavior and the temperature at which the spectral gap opens.

Beyond the implications for the problem of disordered magnets, our data demonstrate the ability to imprint phase-coherent information in a chemically homogeneous bulk magnetic material, using frequency as a label. This means that solid magnets may yet have a future in quantum information processing applications where coherent spin oscillations are actively manipulated to implement computations (23). The necessary next step would involve entangling the states, a possibility

that can be explored in $\text{Li}(\text{Ho},\text{Y})\text{F}_4$, because for this material an external transverse field readily produces quantum mixing (16, 24).

References and Notes

1. J. M. Kikkawa, I. P. Smorchkova, N. Samarth, D. D. Awschalom, *Science* **277**, 1284 (1997).
2. J. M. Lutinger, L. Tisza, *Phys. Rev.* **70**, 954 (1947).
3. D. H. Reich et al., *Phys. Rev. B* **42**, 4631 (1990).
4. D. H. Reich, T. F. Rosenbaum, G. Aeppli, *Phys. Rev. Lett.* **59**, 1969 (1987).
5. A. Aharony, M. J. Stephen, *J. Phys. C* **14**, 1665 (1981).
6. A pair of induction coils was used in a standard gradiometer configuration, and the magnetization oscillations were measured using a digital lock-in technique. For sufficiently small h_{ac} , the oscillation amplitude is linear in h_{ac} and the constant of proportionality is a complex number representing the magnetic susceptibility, $\chi(f) = \chi'(f) + i\chi''(f)$; the real and imaginary parts represent the in-phase and dissipative out-of-phase signals, respectively. Measuring frequencies f ranged between 0.1 and 100 kHz. Field amplitudes less than 0.05 Oe were required for linear response. The $\text{LiHo}_x\text{Y}_{1-x}\text{F}_4$ material was chosen for its known purity and homogeneity. The lattice constants vary by less than 0.01% between $x = 0$ and 1, helping ensure a statistically random distribution of the Ho ions. We have explicitly ruled out chemical segregation effects on the basis of neutron scattering studies, which find no evidence for nuclear short-range order due to clustering.
7. P. Debye, *Polar Molecules* (Chemical Catalogue, New York, 1929), p. 90.
8. P. K. Dixon, L. Wu, S. R. Nagel, B. D. Williams, J. P. Carini, *Phys. Rev. Lett.* **65**, 1108 (1990).
9. Long-time relaxation in dielectric glasses has been attributed to the opening of a dipole gap [D. J.

- Salvino, S. Rogge, B. Tigner, D. D. Osheroff, *Phys. Rev. Lett.* **73**, 268 (1994)].
10. A. L. Burin, *J. Low Temp. Phys.* **100**, 309 (1995).
11. See, for example, W. E. Moerner, Ed., *Persistent Spectral Hole Burning: Science and Applications* (Springer-Verlag, New York, 1988).
12. B. Scheiner, R. Bohmer, A. Loidl, R. V. Chamberlin, *Science* **274**, 752 (1996).
13. R. V. Chamberlin, *Phys. Rev. Lett.* **83**, 5134 (1999).
14. L. C. Cugliandolo, J. L. Iguain, *Phys. Rev. Lett.* **85**, 3448 (2000).
15. For a discussion of ringing oscillations in charge-density-wave systems, see S. N. Coppersmith and P. B. Littlewood [*Phys. Rev. B* **31**, 4049 (1985)].
16. J. Brooke, T. F. Rosenbaum, G. Aeppli, *Nature* **413**, 610 (2001).
17. K. Binder, A. P. Young, *Rev. Mod. Phys.* **58**, 801 (1986).
18. J. A. Mydosh, *Spin Glasses: An Experimental Introduction* (Taylor & Francis, London, 1993).
19. L. Gammaitoni, P. Hanggi, F. Marchesoni, *Rev. Mod. Phys.* **70**, 223 (1998).
20. A. Simon, A. Libchaber, *Phys. Rev. Lett.* **68**, 3375 (1992).
21. R. Giraud, W. Wernsdorfer, A. M. Tkachuk, D. Mailly, B. Barbara, *Phys. Rev. Lett.* **87**, 57203 (2001).
22. P. E. Hansen, T. Johansson, R. Nevald, *Phys. Rev. B* **12**, 5315 (1976).
23. N. A. Gershenfeld, I. L. Chuang, *Science* **275**, 350 (1997).
24. W. Wu, B. Ellman, T. F. Rosenbaum, G. Aeppli, D. H. Reich, *Phys. Rev. Lett.* **67**, 2076 (1991).
25. We have benefited greatly from discussions with J. Brooke, P. Chandra, S. Coppersmith, and S. Girvin. The work at the University of Chicago was supported primarily by the Materials Research Science and Engineering Centers Program of NSF under award DMR-9808595.

11 February 2002; accepted 2 May 2002

Antibody-Based Bio-Nanotube Membranes for Enantiomeric Drug Separations

Sang Bok Lee,¹ David T. Mitchell,¹ Lacramioara Trofin,¹ Tarja K. Nevanen,² Hans Söderlund,² Charles R. Martin^{1*}

Synthetic bio-nanotube membranes were developed and used to separate two enantiomers of a chiral drug. These membranes are based on alumina films that have cylindrical pores with monodisperse nanoscopic diameters (for example, 20 nanometers). Silica nanotubes were chemically synthesized within the pores of these films, and an antibody that selectively binds one of the enantiomers of the drug was attached to the inner walls of the silica nanotubes. These membranes selectively transport the enantiomer that specifically binds to the antibody, relative to the enantiomer that has lower affinity for the antibody. The solvent dimethyl sulfoxide was used to tune the antibody binding affinity. The enantiomeric selectivity coefficient increases as the inside diameter of the silica nanotubes decreases.

Drugs that are produced as racemic mixtures normally contain only one enantiomer that is efficacious (1), and there is increasing pressure on the pharmaceutical industry to market enan-

tiomerically pure drugs (2). One approach for obtaining an enantiomerically pure drug is to effect a chiral separation, typically by means of a chromatographic method (3, 4). An alternative enantioseparation strategy entails the use of a synthetic membrane to selectively transport the desired enantiomer from the racemic mixture into a receiver solution on the other side of the membrane (5–10). This requires that an enantioselective molecular recognition agent be incorporated into the membrane, and there are a

¹Department of Chemistry and Center for Research at the Bio/Nano Interface, University of Florida, Gainesville, FL 32611–7200, USA. ²VTT Biotechnology, Post Office Box 1500, FIN-02044 VTT, Espoo, Finland.

*To whom correspondence should be addressed. E-mail: crmartin@chem.ufl.edu